Letters

Discovery of a second-site *nia2* mutation in the background of multiple *Arabidopsis* PIF-related mutants containing the *pif3-3* allele

Nitrogen (N) is one of the most needed mineral nutrients for plants due to its involvement in the biosynthesis of proteins, nucleic acids, and other essential cellular components such as chlorophyll and phytohormones (Crawford, 1995). Plants can extract N from the soil in a variety of forms, but nitrate (NO_3^-) represents the predominant source of N in most agricultural soils (Crawford & Forde, 2002). Nitrate is taken up by the root via NO_3^- transporters belonging to the NITRATE TRANSPORTER1/PEPTIDE TRANSPORTER FAMILY (NRT1/NPF) and NRT2 families (Wang *et al.*, 2012; Krapp *et al.*, 2014). Subsequently, most NO_3^- is translocated to shoot tissue to be reduced by nitrate reductase (NR) to nitrite (NO_2^-), which is converted into ammonium (NH_4^+) before being incorporated into the amino acid pool via the action of the glutamine synthase/glutamine oxoglutarate aminotransferase or glutamate synthase (GS/GOGAT) pathway (Campbell, 1999). As the enzyme catalysing the rate-limiting step of NO_3^- assimilation, and a major enzymatic source for the biosynthesis of the nitric oxide (NO) signalling molecule (Chamizo-Ampudia *et al.*, 2017; Khan *et al.*, 2023), NR is under extensive regulation at both transcriptional and post-transcriptional levels in response to various endogenous and environmental factors (e.g. Park *et al.*, 2011; Lambeck *et al.*, 2012; Konishi & Yanagisawa, 2013; Marchive *et al.*, 2013; Creighton *et al.*, 2017; Jamieson *et al.*, 2022). Among them, light, in part through activating sugar assimilation, tightly regulates NR activity because photosynthesis provides the expensive reducing energy required for NO_3^- reduction and needs to be coordinated with NO_3^- metabolism to maintain the carbon (C)/N metabolic balance (Hoff *et al.*, 1994; Baslam *et al.*, 2020). However, the molecular mechanism of how light signalling directly modulates NO_3^- metabolism remains largely elusive.

PHYTOCHROME-INTERACTING FACTORs (PIFs) are basic helix–loop–helix (bHLH) transcription factors that negatively regulate light responses, and are degraded upon the activation of the phytochrome (phy) photoreceptors (Bae & Choi, 2008; Leivar & Quail, 2011; Xu *et al.*, 2015). Moreover, accumulating evidence has demonstrated that PIFs are also targeted by other environmental (e.g. temperature) and developmental (e.g. phytohormones) signals to modulate plant responses, making them central hubs that integrate external stimuli to downstream biological activities (Balcerowicz, 2020; Sanchez *et al.*, 2020). Therefore, we investigated whether PIFs additionally play a role in regulating NO_3^- metabolism in the model plant *Arabidopsis thaliana*.

In this study, we used plant chlorate resistance to assess NO_3^- metabolic capacity (see Supporting Information Notes S1 for Methods and materials). Chlorate is a NO_3^- chemical analogue that can be taken up by NO_3^- transporters and reduced by NR to chlorite, which is toxic to plants and causes leaf chlorosis (Wilkinson & Crawford, 1991; Tsay *et al.*, 1993; Wang & Crawford, 1996). Under our growth conditions, *Arabidopsis nrt1.1* (lacking the dual-affinity NO_3^- transporter NRT1.1) and *chl3-5* (lacking the major isoform of NR, NIA2, which accounts for 80–90% of total NR activity) mutants were resistant to chlorate toxicity (Fig. S1; Wilkinson & Crawford, 1991; Tsay *et al.*, 1993), whereas the *nrt2.1 nrt2.2* (lacking two high-affinity NO_3^- transporters NRT2.1 and NRT2.2) and *nia1-4* (lacking the minor NR isoform, NIA1) were not (Fig. S1). Next, given that PIFs have both shared and distinct regulatory roles (Jeong & Choi, 2013), we tested the chlorate response of the sextuple mutant *pqp6p7* (*pif1-1 pif3-3 pif4-2 pif5-3 pif6-2 pif7-1*), which lacks six of the eight PIFs, thus reducing the risk of potential PIF functional redundancy masking any mutant phenotype. Compared with wild-type (WT), *pqp6p7* plants displayed significantly less leaf chlorosis caused by chlorate toxicity (Fig. 1a,b), suggesting that NO_3^- metabolism was compromised in this mutant. Since the *pqp6p7* mutant was generated by crossing the quadruple *pifq* mutant (*pif1-1 pif3-3 pif4-2 pif5-3*) with *pif6-2* and *pif7-1*, we attempted to narrow down the causal mutation by treating these mutants with chlorate. Although a moderate level of chlorate resistance was observed for *pif7-1*, only *pifq* mutant plants exhibited a comparable level of chlorate resistance to *pqp6p7* (Fig. 1c). Finally, we subjected the individual *pif* mutants that makeup *pifq* to chlorate treatment and found that *pif3-3* exhibited chlorate resistance comparable with that of *pifq* and *pqp6p7* (Fig. 1d), suggesting that the resistance originated from there.

Since chlorate resistance can be attributed to a root-dependent deficiency in NO_3^-/chlorate uptake, or a shoot-dependent deficiency in NO_3^-/chlorate reduction, or both, we speculated that grafting might provide useful insight into the mechanisms of modified chlorate responses exhibited by mutants. As positive controls, we demonstrated that the graft chimaeras with WT shoot on *nrt1.1* root (WT/*nrt1.1*) and *chl3-5* shoot on WT root (*chl3-5*/WT) were resistant to chlorate, whereas the reciprocal graft chimaeras (*nrt1.1*/WT and WT/*chl3-5*) were as sensitive to chlorate toxicity as the WT/WT controls (Fig. S2a,b). Subsequently, grafting was performed between WT and *pif3-3* mutant plants. Among the resultant chimaeras, only those with a *pif3-3* mutant shoot (*pif3-3*/*pif3-3* and *pif3-3*/WT) were resistant to chlorate (Fig. 2a), suggesting a clear shoot-dependency of the chlorate resistance originating from the *pif3-3* mutant.

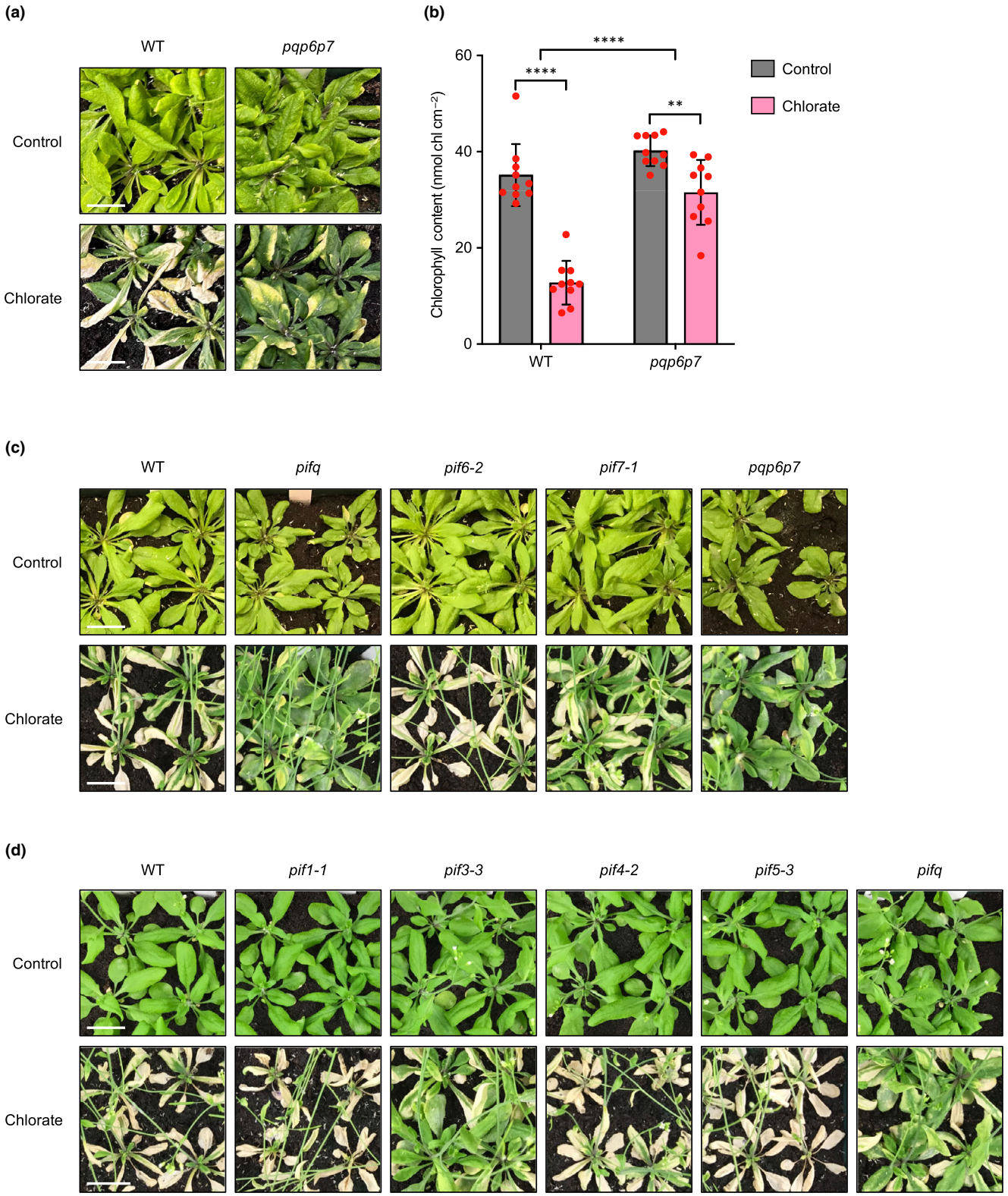

Fig. 1 *pif3-3* and higher-order mutants containing the *pif3-3* allele exhibit resistance to chlorate toxicity. (a) Chlorate responses of wild-type (WT) and *pqp6p7* plants. Four-week-old plants grown on soil were treated with dH_2O (control) or 1.5 mM chlorate every 5 d. When necessary, bolt stems were removed for ease of viewing. Bars, 2 cm. (b) Mean leaf chlorophyll contents, genotypes as shown, red dots indicate individual values ($n = 10$), error bars indicate SD. Statistical analysis was performed with two-way analysis of variance (ANOVA): **, $P \leq 0.01$; ****, $P \leq 0.0001$. (c) Chlorate responses of WT, *pifq*, *pif6-2*, *pif7-1*, and *pqp6p7* plants. Four-week-old plants grown on soil were treated with dH_2O (control) or 1.5 mM chlorate every 5 d. When necessary, bolt stems were removed for ease of viewing. Bars, 2 cm. (d) Chlorate responses of WT, *pif1-1*, *pif3-3*, *pif4-2*, *pif5-3*, and *pifq* plants. Four-week-old plants grown on soil were treated with dH_2O (control) or 1.5 mM chlorate every 5 d. When necessary, bolt stems were removed for ease of viewing. Bars, 2 cm.

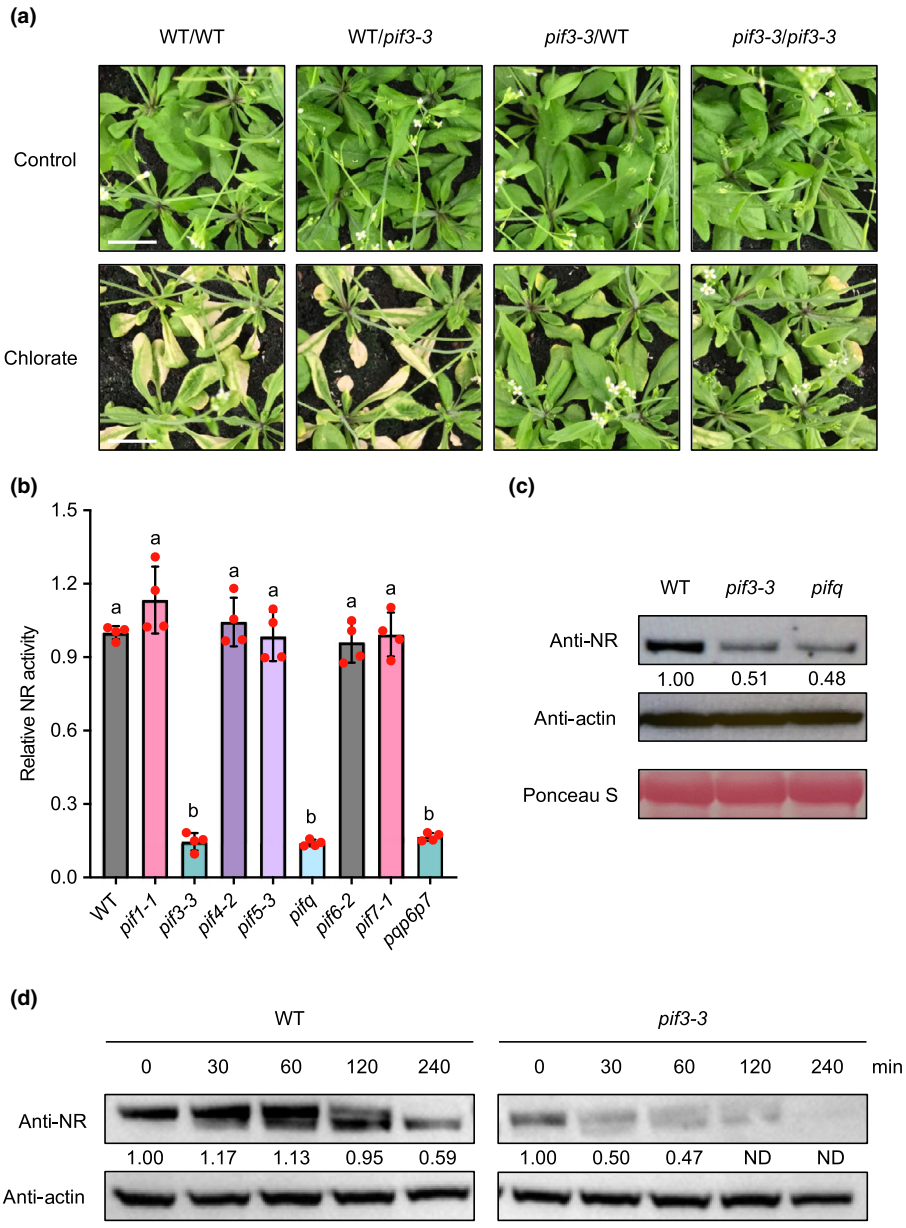

Fig. 2 Shoot-dependent deficiency in nitrate reductase (NR) activity underlies *pif3-3*-conferred chlorate resistance. (a) Chlorate responses of graft chimaeras made by exchanging shoots and roots of wild-type (WT) and *pif3-3* mutant plants. The graft chimaeras are labelled as shoot genotype/root genotype. All graft chimaeras were constructed at seedling stage before being transplanted to soil. Four-week-old plants were treated with dH_2O (control) or 1.5 mM chlorate every 5 d. When necessary, bolt stems were removed for ease of viewing. Bars, 2 cm. (b) Mean relative shoot NR activity of WT and PHYTOCHROME-INTERACTING FACTOR (PIF)-related mutants. Red dots indicate individual values ($n = 4$), error bars indicate SD, and different letters (a, b) indicate significant differences (one-way analysis of variance (ANOVA) with Tukey's test). (c) Abundance of immuno-detected NR in WT, *pif3-3*, and *pifq* plant extracts, quantified against Actin control (arbitrarily set at 1.00 for WT). Ponceau S staining serves as loading control. (d) Destruction rates of endogenous NR in WT and *pif3-3* plant extracts, with immunodetectable NR quantified against Actin control (arbitrarily set at 1.00 for time point 0). ND, band not detected.

Accordingly, compared with WT and the other *pif* mutants, mutants containing the *pif3-3* allele exhibited a drastically reduced NR activity (Fig. 2b). Despite the lack of a detectable difference in the transcript levels of the two NR genes, *NIA1* and *NIA2* (Fig. S2c, d), the reduction in NR activity was reflected by a lower NR protein abundance in *pif3-3* and *pifq* than that of WT (Fig. 2c). Cell-free degradation assay showed that the rate of NR protein degradation was accelerated in *pif3-3* compared with WT, indicating a reduction in NR protein stability (Fig. 2d).

The *pif3-3* allele was generated by fast neutron mutagenesis, which induced a 2.5-kb deletion in the promoter region of *PIF3* that resulted in no detectable transcript of this gene (Fig. S3a; Monte *et al.*, 2004; see Table S1 for primers used in this study). Two other *pif3* mutant alleles, *pif3-1* and *pif3-2*, contain T-DNA insertions in the fourth intron of *PIF3* and produce truncated transcripts encoding a potential protein lacking a functional bHLH domain (Fig. S3a; Monte *et al.*, 2004). Intriguingly, unlike *pif3-3*, the *pif3-1* and *pif3-2* mutants exhibited similar chlorate responses and NR activities to WT (Figs 3a, S3b). To rule out the possibility that the truncated transcripts produced by *pif3-1* and *pif3-2* were functional in maintaining a WT level of NR activity, we generated our own *pif3* mutants using clustered regularly interspaced palindromic repeats (CRISPR)/CRISPR-associated protein 9 (Cas9) that introduced frame shifts early in the gene (Fig. S3c), and confirmed that their NR activity was not affected by the mutations (Fig. 3b). Finally, we showed that the overexpression of *PIF3* in the *pif3-3* mutant background led to an elongated hypocotyl phenotype characteristic of PIF over-accumulation, but did not revert the repression of NR activity (Figs 3c, S3d,e). Collectively, we conclude that the observed low NR activity in *pif3-3* is not due to the mutation in *PIF3 per se*, but rather to another mutation in the background, presumably caused by fast neutron bombardment.

New Phytologist

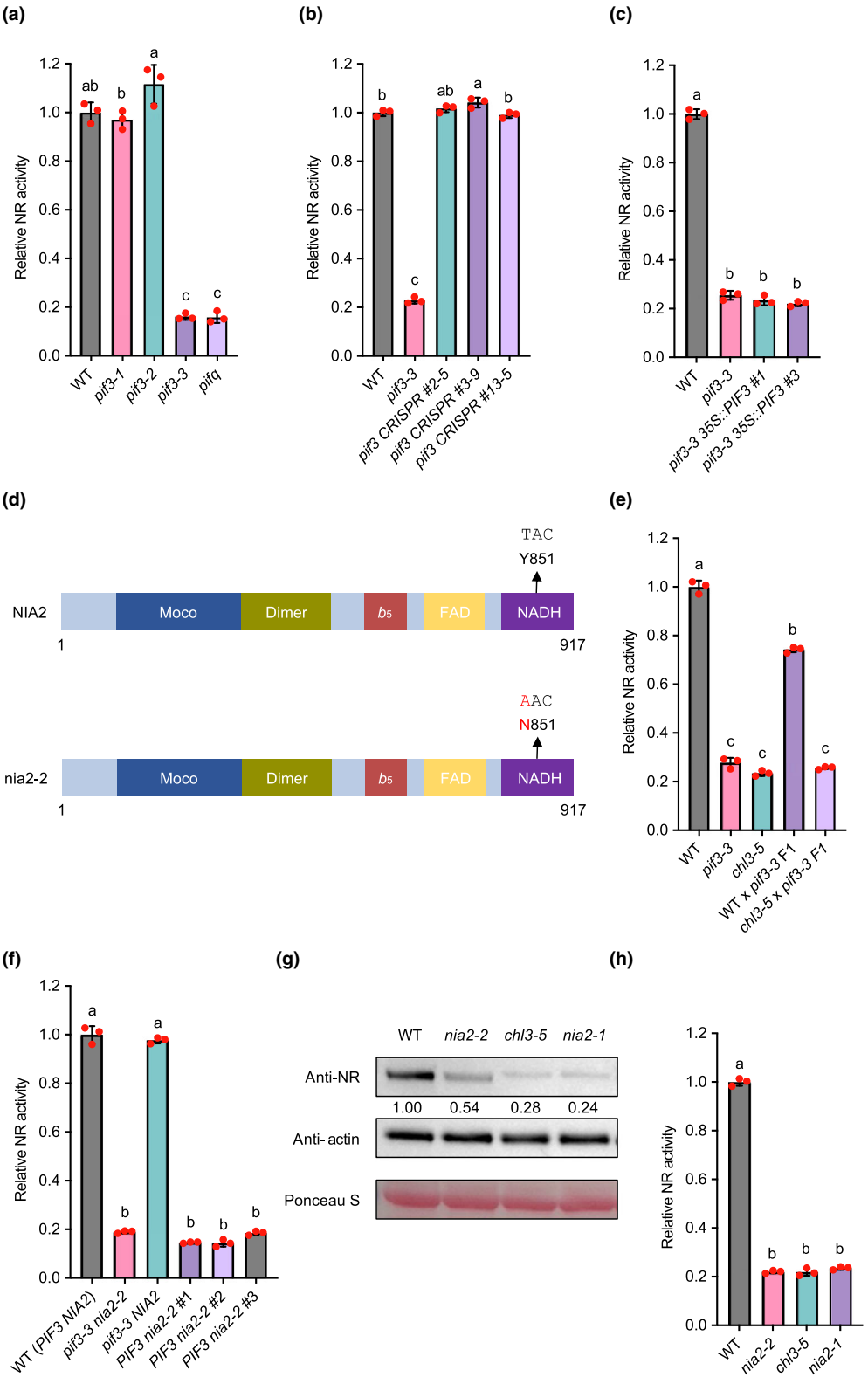

In order to identify the actual mutation in the background of *pif3-3* that is responsible for its chlorate resistance and reduced NR activity, whole-genome sequencing analysis was performed for the *pif3-3* single mutant. We identified multiple single nucleotide variants (SNVs) and INDELs (insertions and deletions) present in the *pif3-3* mutant (Datasets S1, S2). Among them, a SNV in the *NIA2*

Fig. 3 *nia2-2* mutation in the background of *pif3-3* is responsible for its compromised nitrate reductase (NR) activity. (a) Mean relative shoot NR activity of wild-type (WT) and PHYTOCHROME-INTERACTING FACTOR (PIF)-related mutants. Red dots indicate individual values ($n = 3$), error bars indicate SD, and different letters (a–c) indicate significant differences (one-way analysis of variance (ANOVA) with Tukey's test). (b) Mean relative shoot NR activity of WT, *pif3-3*, and independent *pif3* mutants generated by clustered regularly interspaced palindromic repeats (CRISPR)/CRISPR-associated protein 9 (Cas9)-mediated genome editing. Red dots indicate individual values ($n = 3$), error bars indicate SD, and different letters (a–c) indicate significant differences (one-way ANOVA with Tukey's test). (c) Mean relative shoot NR activity of WT, *pif3-3*, and independent *pif3 35S::PIF3* Complementation lines. Red dots indicate individual values ($n = 3$), error bars indicate SD, and different letters (a, b) indicate significant differences (one-way ANOVA with Tukey's test). (d) *nia2-2* encodes a mutant nia2 protein with the Y851N amino acid substitution. Conserved subdomains of NIA2 are as indicated (Chamizo-Ampudia *et al*., 2017). (e) Mean relative shoot NR activity of WT, *pif3-3*, *chl3-5*, and the F1 progeny made from crossing *pif3-3* with either WT or *chl3-5*. Red dots indicate individual values ($n = 3$), error bars indicate SD, and different letters (a–c) indicate significant differences (one-way ANOVA with Tukey's test). (f) Mean relative shoot NR activity of WT (*PIF3 NIA2*), *pif3-3 nia2-2*, *pif3-3 NIA2*, and independent *PIF3 nia2-2* plants. Red dots indicate individual values ($n = 3$), error bars indicate SD, and different letters (a, b) indicate significant differences (one-way ANOVA with Tukey's test). (g) Abundance of immuno-detected NR in WT, *nia2-2*, *chl3-5*, and *nia2-1* plant extracts, quantified against Actin control (arbitrarily set at 1.00 for WT). Ponceau S staining serves as loading control. (h) Mean relative shoot NR activity of WT, *nia2-2*, *chl3-5*, and *nia2-1*. Red dots indicate individual values ($n = 3$), error bars indicate SD, and different letters (a, b) indicate significant differences (one-way ANOVA with Tukey's test).

gene of *pif3-3* led to a single amino acid substitution (Y851N) in the NADH-binding domain of the NIA2 protein (Fig. 3d). To confirm that this mutant *nia2* allele (which we name *nia2-2*) compromised NR activity, we performed allelism tests by crossing *pif3-3* (with *nia2-2* in the background) with known *nia2* loss-of-function mutants, *chl3-5* (deletion of the entire *NIA2* gene) and *nia2-1* (T-DNA insertion *nia2* mutant), respectively. The F1 progeny from these crosses exhibited a similar level of NR activity as the parental *pif3-3 nia2-2* and *chl3-5* or *nia2-1* mutants (Figs 3e, S3f). On the contrary, F1 plants from crossing *pif3-3 nia2-2* with WT had an intermediate level of NR activity (Figs 3e, S3f), which is consistent with the fact that the *NIA2* gene is haploinsufficient (Wilkinson & Crawford, 1991). The F1 *PIF3*/*pif3-3 NIA2*/*nia2-2* heterozygous plants were allowed to self, and from the F2 population, we isolated individuals with only one of these two mutations, that is *pif3-3 NIA2* and *PIF3 nia2-2*. NR activity assay revealed that the *nia2-2* mutation is solely responsible for the decreased NR activity in the original *pif3-3* mutant and without it in the background, independent *pif3-3 NIA2* lines isolated from the F2 population of a WT (*PIF3 NIA2*) × *pif3-3 nia2-2* cross do not have a detectably different NR activity compared with WT (*PIF3 NIA2*, Fig. 3f).

The Y851 residue locates within the C terminus domain of the NIA2 protein that binds to NADH, which provides the electron essential for NO_3^- reduction (Campbell & Kinghorn, 1990). Furthermore, Y851 was found to be highly conserved in NIA orthologs across the plant kingdom from green algae to angiosperms, except for one of the two NIA homologues in *Physcomitrium patens*, whose corresponding site was occupied by a chemically similar phenylalanine (F) residue (Fig. S3g). Therefore, it is reasonable to speculate that Y851 at this position confers an important function, and substituting it with an asparagine (N) that is both structurally and chemically distinct from Y probably destabilises the protein (Fig. 2c,d). However, the protein abundance of NR in *nia2-2* was still higher than that in *chl3-5* or *nia2-1*, even though the NR activity was indistinguishable between the three *nia2* mutants (Fig. 3g,h). Therefore, the Y851N substitution might additionally disrupt normal NR enzymatic activity.

Taken together, we report here the discovery of a hidden *nia2-2* mutation in multiple mutants containing the *pif3-3* allele and show that *nia2-2* confers reduced NR activity, thus compromising NO_3^- metabolism. This finding indirectly suggests that light-mediated regulation of NR activity is unlikely to involve most of the PIF family proteins, although the mild chlorate resistance phenotype conferred by *pif7-1* is worth exploring in future studies. The characterisation of the *nia2-2* mutation also highlights the functional importance of Y851 in maintaining NR protein stability and enzymatic activity and provides a valuable mutant resource for studying NR functions. Lastly, we present a pipeline that can be referred to when studying a regulatory component of NO_3^- metabolism. Specifically, we highlight the use of grafting as a novel and effective approach for spatially separating and distinguishing the effect on NO_3^- uptake in the root and NO_3^- assimilation in the shoot.

The *pif3-3* mutant and higher-order mutants containing the *pif3-3* allele (e.g. *pifq* and *pqp6p7*) have been widely used to study PIF functions (e.g. Jiang *et al*., 2020; Bernula *et al*., 2021; Yoo *et al*., 2021; Piskurewicz *et al*., 2023; Sng *et al*., 2023). The identification of the hidden *nia2-2* mutation revealed here might render it worthwhile re-examining the alternative interpretation that some of the reported mutant phenotypes were due to the deficiency in N metabolism and/or NO production, especially for any studies investigating the crosstalk between the PIF and NO signalling pathways (Lozano-Juste & León, 2011; Bai *et al*., 2014). We were initially surprised that the *nia2-2* allele somehow evaded being eliminated through multiple rounds of crossing and persisted in the quadruple and sextuple *pif* mutants (especially considering that the original *pif3-3* mutant was outcrossed twice with Col-0 following its isolation, Monte *et al*., 2004). There is clearly not an absolute linkage between the *PIF3* and *NIA2* genes because we have successfully separated the two mutant alleles in this study. However, the fact that they reside on the same chromosome (PIF3: AT1G09530; NIA2: AT1G37130; Fig. S3h) suggests that they might be partially linked, and therefore, the mutant alleles may not assort completely independently during meiosis.

Forward genetics is a powerful approach for understanding gene function underlying a particular mutant phenotype induced by random mutagenesis in an unbiased manner that requires no prior knowledge about the gene of interest (Peters *et al*., 2003). However, random mutagenesis poses the risk of generating second-site mutations that are responsible for the observed phenotype but are overlooked, which led to a plethora of recent publications unmasking these mutations in previously reported mutants (e.g. Bennett *et al*., 2006; Westphal *et al*., 2008; Enders *et al*., 2015; Gao *et al*., 2015; Kriegel *et al*., 2015; Wu *et al*., 2015; Yoshida *et al*., 2018; Vlad & Langdale, 2022; Yu *et al*., 2023). Therefore, we wish to

remind the science community to not discount the possibility of a mutant material harbouring secondary mutations in the background, which seems to be particularly common for those generated from nonspecific mutagenesis. If possible, the use of other independent mutant alleles should always be included in their studies. Alternatively, complementation tests (using complete complementation gene constructs) can be performed to validate gene functions.

Acknowledgements

Funding (SL and XF) was from the National Natural Science Foundation of China (grants 32122065 and 32020103004), and (NPH) from UKRI (BBSRC) grant BB/S013741/1. NPH gratefully acknowledges research funding support from St John's College, Oxford. We thank Francesco Licausi for providing the *pqp6p7* mutant, Charles Melnyk for the protocol of grafting with *Arabidopsis*, and Paul Javis for providing the pEarlyGate202 plasmid.

Competing interests

None declared.

Author contributions

NPH, EJB and ZJ conceived the project and designed the experiments. ZJ performed most of the experiments and wrote the manuscript. EJB analysed the whole-genome sequencing data. SL assisted with the construction of plant transformants. XF provided creative input. All authors discussed the results and contributed to the manuscript.

ORCID

Eric J. Belfield https://orcid.org/0000-0003-0892-100X
Xiangdong Fu https://orcid.org/0000-0001-9285-7543
Nicholas P. Harberd https://orcid.org/0000-0002-7634-3902
Zhe Ji https://orcid.org/0000-0002-0651-2598
Shan Li https://orcid.org/0000-0003-2837-9027

Data availability

All data generated in this study are included in the main text and Supporting Information of this article. The Illumina DNA sequencing data files from this study have been submitted to the NCBI Sequence Read Archive (SRA; http://www.ncbi.nlm.nih.gov/sra) under accession no. SRR26298495.

Zhe Ji[1,2]*, Eric J. Belfield[1], Shan Li[2,3], Xiangdong Fu[2,4,5] and Nicholas P. Harberd[1]*

[1]Department of Biology, University of Oxford, Oxford, OX1 3RB, UK;
[2]State Key Laboratory of Plant Cell and Chromosome Engineering, Institute of Genetics and Developmental Biology, Chinese Academy of Sciences, Beijing, 100101, China;
[3]National Key Laboratory of Crop Genetics & Germplasm Enhancement and Utilization, Nanjing Agricultural University, Nanjing, 210095, China;
[4]College of Life Sciences, University of Chinese Academy of Sciences, Beijing, 100049, China;
[5]New Cornerstone Science Laboratory, Beijing, 100101, China
(*Authors for correspondence: email nicholas.harberd@biology.ox.ac.uk (NPH); zhe.ji@biology.ox.ac.uk (ZJ))

References

Bae G, Choi G. 2008. Decoding of light signals by plant phytochromes and their interacting proteins. *Annual Review of Plant Biology* **59**: 281–311.
Bai SL, Yao T, Li MM, Guo XM, Zhang YC, Zhu SW, He YK. 2014. PIF3 is involved in the primary root growth inhibition of Arabidopsis induced by nitric oxide in the light. *Molecular Plant* **7**: 616–625.
Balcerowicz M. 2020. PHYTOCHROME-INTERACTING FACTORS at the interface of light and temperature signalling. *Physiologia Plantarum* **169**: 347–356.
Baslam M, Mitsui T, Sueyoshi K, Ohyama T. 2020. Recent advances in carbon and nitrogen metabolism in C_3 plants. *International Journal of Molecular Sciences* **22**: 318.
Bennett T, Sieberer T, Willett B, Booker J, Luschnig C, Leyser O. 2006. The Arabidopsis MAX pathway controls shoot branching by regulating auxin transport. *Current Biology* **16**: 553–563.
Bernula P, Pettko-Szandtner A, Hajdu A, Kozma-Bognar L, Josse EM, Adam E, Nagy F, Viczian A. 2021. SUMOylation of PHYTOCHROME INTERACTING FACTOR 3 promotes photomorphogenesis in *Arabidopsis thaliana*. *New Phytologist* **229**: 2050–2061.
Campbell WH. 1999. Nitrate reductase structure, function and regulation: bridging the gap between biochemistry and physiology. *Annual Review of Plant Physiology and Plant Molecular Biology* **50**: 277–303.
Campbell WH, Kinghorn KR. 1990. Functional domains of assimilatory nitrate reductases and nitrite reductases. *Trends in Biochemical Sciences* **15**: 315–319.
Chamizo-Ampudia A, Sanz-Luque E, Llamas A, Galvan A, Fernandez E. 2017. Nitrate reductase regulates plant nitric oxide homeostasis. *Trends in Plant Science* **22**: 163–174.
Crawford NM. 1995. Nitrate: nutrient and signal for plant growth. *Plant Cell* **7**: 859–868.
Crawford NM, Forde BG. 2002. Molecular and developmental biology of inorganic nitrogen nutrition. *Arabidopsis Book* **1**: e0011.
Creighton MT, Sanmartin M, Kataya ARA, Averkina IO, Heidari B, Nemie-Feyissa D, Sanchez-Serrano JJ, Lillo C. 2017. Light regulation of nitrate reductase by catalytic subunits of protein phosphatase 2A. *Planta* **246**: 701–710.
Enders TA, Oh S, Yang ZB, Montgomery BL, Strader LC. 2015. Genome sequencing of Arabidopsis abp1-5 reveals second-site mutations that may affect phenotypes. *Plant Cell* **27**: 1820–1826.
Gao YB, Zhang Y, Zhang D, Dai XH, Estelle M, Zhao YD. 2015. Auxin binding protein 1 (ABP1) is not required for either auxin signaling or Arabidopsis development. *Proceedings of the National Academy of Sciences, USA* **112**: 2275–2280.
Hoff T, Truong HN, Caboche M. 1994. The use of mutants and transgenic plants to study nitrate assimilation. *Plant, Cell & Environment* **17**: 489–506.
Jamieson F, Ji Z, Belfield EJ, Ding ZJ, Zheng SJ, Harberd NP. 2022. Ethylene signaling modulates *Arabidopsis thaliana* nitrate metabolism. *Planta* **255**: 94.
Jeong J, Choi G. 2013. Phytochrome-interacting factors have both shared and distinct biological roles. *Molecules and Cells* **35**: 371–380.
Jiang B, Shi Y, Peng Y, Jia Y, Yan Y, Dong X, Li H, Dong J, Li J, Gong Z *et al.* 2020. Cold-induced CBF-PIF3 interaction enhances freezing tolerance by stabilizing the phyB thermosensor in Arabidopsis. *Molecular Plant* **13**: 894–906.
Khan M, Ali S, Al Azzawi TNI, Yun BW. 2023. Nitric oxide acts as a key signaling molecule in plant development under stressful conditions. *International Journal of Molecular Sciences* **24**: 4782.
Konishi M, Yanagisawa S. 2013. Arabidopsis NIN-like transcription factors have a central role in nitrate signalling. *Nature Communications* **4**: 1617.

Krapp A, David LC, Chardin C, Girin T, Marmagne A, Leprince AS, Chaillou S, Ferrario-Mery S, Meyer C, Daniel-Vedele F. 2014. Nitrate transport and signalling in Arabidopsis. *Journal of Experimental Botany* **65**: 789–798.

Kriegel A, Andres Z, Medzihradszky A, Kruger F, Scholl S, Delang S, Patir-Nebioglu MG, Gute G, Yang H, Murphy AS *et al.* 2015. Job sharing in the endomembrane system: vacuolar acidification requires the combined activity of V-ATPase and V-PPase. *Plant Cell* **27**: 3383–3396.

Lambeck IC, Fischer-Schrader K, Niks D, Roeper J, Chi JC, Hille R, Schwarz G. 2012. Molecular mechanism of 14-3-3 protein-mediated inhibition of plant nitrate reductase. *Journal of Biological Chemistry* **287**: 4562–4571.

Leivar P, Quail PH. 2011. PIFs: pivotal components in a cellular signaling hub. *Trends in Plant Science* **16**: 19–28.

Lozano-Juste J, León J. 2011. Nitric oxide regulates DELLA content and PIF expression to promote photomorphogenesis in Arabidopsis. *Plant Physiology* **156**: 1410–1423.

Marchive C, Roudier F, Castaings L, Brehaut V, Blondet E, Colot V, Meyer C, Krapp A. 2013. Nuclear retention of the transcription factor NLP7 orchestrates the early response to nitrate in plants. *Nature Communications* **4**: 1713.

Monte E, Tepperman JM, Al-Sady B, Kaczorowski KA, Alonso JM, Ecker JR, Li X, Zhang Y, Quail PH. 2004. The phytochrome-interacting transcription factor, PIF3, acts early, selectively, and positively in light-induced chloroplast development. *Proceedings of the National Academy of Sciences, USA* **101**: 16091–16098.

Park BS, Song JT, Seo HS. 2011. Arabidopsis nitrate reductase activity is stimulated by the E3 SUMO ligase AtSIZ1. *Nature Communications* **2**: 400.

Peters JL, Cnudde F, Gerats T. 2003. Forward genetics and map-based cloning approaches. *Trends in Plant Science* **8**: 484–491.

Piskurewicz U, Sentandreu M, Iwasaki M, Glauser G, Lopez-Molina L. 2023. The Arabidopsis endosperm is a temperature-sensing tissue that implements seed thermoinhibition through phyB. *Nature Communications* **14**: 1202.

Sanchez SE, Rugnone ML, Kay SA. 2020. Light perception: a matter of time. *Molecular Plant* **13**: 363–385.

Sng BJR, Vu KV, Choi IKY, Chin HJ, Jang IC. 2023. LONG HYPOCOTYL IN FAR-RED 1 mediates a trade-off between growth and defence under shade in Arabidopsis. *Journal of Experimental Botany* **74**: 3560–3578.

Tsay YF, Schroeder JI, Feldmann KA, Crawford NM. 1993. The herbicide sensitivity gene CHL1 of Arabidopsis encodes a nitrate-inducible nitrate transporter. *Cell* **72**: 705–713.

Vlad D, Langdale JA. 2022. DEFECTIVELY ORGANIZED TRIBUTARIES 5 is not required for leaf venation patterning in *Arabidopsis thaliana*. *The Plant Journal* **112**: 451–459.

Wang RC, Crawford NM. 1996. Genetic identification of a gene involved in constitutive, high-affinity nitrate transport in higher plants. *Proceedings of the National Academy of Sciences, USA* **93**: 9297–9301.

Wang YY, Hsu PK, Tsay YF. 2012. Uptake, allocation and signaling of nitrate. *Trends in Plant Science* **17**: 458–467.

Westphal L, Scheel D, Rosahl S. 2008. The coi1-16 mutant harbors a second site mutation rendering PEN2 nonfunctional. *Plant Cell* **20**: 824–826.

Wilkinson JQ, Crawford NM. 1991. Identification of the Arabidopsis Chl3 gene as the nitrate reductase structural gene Nia2. *Plant Cell* **3**: 461–471.

Wu YR, Li YQ, Liu YC, Xie Q. 2015. Cautionary notes on the usage of abi1-2 and abi1-3 mutants of Arabidopsis ABI1 for functional studies. *Molecular Plant* **8**: 335–338.

Xu X, Paik I, Zhu L, Huq E. 2015. Illuminating progress in phytochrome-mediated light signaling pathways. *Trends in Plant Science* **20**: 641–650.

Yoo CY, He JM, Sang Q, Qiu YJ, Long LY, Kim RJA, Chong EG, Hahm J, Morffy N, Zhou P *et al.* 2021. Direct photoresponsive inhibition of a p53-like transcription activation domain in PIF3 by Arabidopsis phytochrome B. *Nature Communications* **12**: 5614.

Yoshida Y, Sarmiento-Manus R, Yamori W, Ponce MR, Micol JL, Tsukaya H. 2018. The Arabidopsis phyB-9 mutant has a second-site mutation in the VENOSA4 gene that alters chloroplast size, photosynthetic traits, and leaf growth. *Plant Physiology* **178**: 3–6.

Yu DM, Dong X, Zou K, Jiang XD, Sun YB, Min ZJ, Zhang LP, Cui HT, Hu JY. 2023. A hidden mutation in the seventh WD40-repeat of COP1 determines the early flowering trait in a set of Arabidopsis myc mutants. *Plant Cell* **35**: 345–350.

Supporting Information

Additional Supporting Information may be found online in the Supporting Information section at the end of the article.

Dataset S1 List of SNVs identified in *pif3-3*.

Dataset S2 List of INDELs identified in *pif3-3*.

Fig. S1 *Arabidopsis* mutants deficient in NO_3^- uptake or NO_3^- assimilation exhibit resistance to chlorate toxicity.

Fig. S2 Validation of grafting as a means of understanding the mechanisms of modified chlorate responses exhibited by mutants.

Fig. S3 *nia2-2* mutation in the background of *pif3-3* is responsible for its compromised NR activity.

Notes S1 Methods and materials.

Table S1 List of primers used in this study.

Please note: Wiley is not responsible for the content or functionality of any Supporting Information supplied by the authors. Any queries (other than missing material) should be directed to the *New Phytologist* Central Office.

Key words: *Arabidopsis*, grafting, mutant, nitrate reductase, PHYTOCHROME-INTERACTING FACTORs (PIFs).

Received, 10 August 2023; accepted, 25 September 2023.